

Pre-inflationary perturbations from closed algebra approach in loop quantum cosmology

Bao-Fei Li^{a,b,*}, Tao Zhu^{a,b,†}, Anzhong Wang^{a,b,‡}, Klaus Kirsten^{c,§}, Gerald Cleaver^{d,¶} and Qin Sheng^{c,**}

^a *Institute for Advanced Physics & Mathematics,
Zhejiang University of Technology, Hangzhou, 310032, China*

^b *GCAP-CASPER, Physics Department, Baylor University,
Waco, TX 76798-7316, USA*

^c *GCAP-CASPER,
Mathematics Department, Baylor University, Waco, TX 76798-7328, USA*

^d *EUCOS-CASPER, Physics Department, Baylor University, Waco, TX 76798-7316, USA*

(Dated: June 7, 2021)

In this paper, the scalar and tensor perturbations in the closed algebra approach of loop quantum cosmology are studied. Instead of the distant past in the contracting phase, we choose the moment at which the initial conditions are imposed to be the silent point, which circumvents the problem due to the signature change in the super-inflationary phase and results in a well-defined Cauchy problem. For the ultraviolet and infrared modes, different approaches are applied in order to obtain analytical solutions with high accuracy. While previous numerical simulations reveal an exponentially divergent power spectrum in the ultraviolet regime, when the initial conditions are imposed in the remote contracting phase, we find a special set of initial conditions at the silent point, which can reproduce results that are consistent with current observations.

I. INTRODUCTION

As a non-perturbative and background-independent approach to quantizing general relativity, loop quantum gravity (LQG) presents a basic framework in which discrete structures of some fundamental geometric quantities, such as areas and volumes, are found at the quantum level [1–3]. However, as LQG is concerned with physics at the Planck scale, it's almost impossible to directly detect the predictions from LQG by any man-made terrestrial experiments in the near future. This makes primordial cosmology an invaluable arena for investigating various aspects of quantum gravity, including testing LQG. In the cosmological settings, due to the homogeneity and isotropy of the Universe, the quantization of cosmology can be studied by a symmetry reduced version of LQG [4, 5]. Although different quantization approaches result in different models and thus distinctive phenomenologies [6–8], in this paper, we will mainly focus on loop quantum cosmology (LQC), which is one of the most developed quantum cosmological theories.

In LQC, the classical singularity in the standard big-bang model is replaced by the quantum bounce due to the pure quantum geometric effects at the Planck scale [9–11]. The pre-inflationary dynamics of LQC has been studied extensively in the literature [12–20, 22–25]. Basically, the background evolution in LQC is symmetric with respect to the bounce, and the slow-roll inflation turns out to be an attractor in a variety of inflationary potentials

when the Universe is sourced by a single scalar field [17–21]. One of the most important unknowns regarding the dynamics of the background in LQC is the way to set initial conditions. In principle, the initial conditions can be set either in the remote past of the contracting phase [13] or at the bounce point when the critical energy density is attained [26]. The most immediate physical consequence resulted from the choice of different initial conditions lies in the duration of the inflationary phase. For example, if the initial conditions are chosen in the prebounce phase, the preferred number of inflationary e-folds is around 140 for the chaotic inflation [13, 17, 18, 23, 24]. Whereas, if the initial conditions are set at the bounce point, the most probable e-folds number can be as large as 10^{12} [25]. Even though, there seems huge differences in the number of inflationary e-folds when different ansatzes for setting initial conditions are employed, these differences are not substantial in the sense that the most probable e-folds number in one ansatz can be the fine-tuned one in the other ansatz. On the other hand, more important differences show up from different approaches to cosmological perturbations.

Up to now, there are at least three different approaches to study the primordial power spectra in LQC, the dressed metric [26–28]¹, closed algebra [34–36] and separate universes [37, 38]. In the dressed metric approach, the background metric is quantized by the loop approach while its perturbative degrees of freedom are quantized following the Fock quantization procedures. As long as the energy density in the perturbations remain small as compared to the Planck energy, the quantum dynam-

* Bao-Fei.Li@baylor.edu

† zhut05@zjut.edu.cn

‡ anzhong_wang@baylor.edu; Corresponding author

§ klaus_kirsten@baylor.edu

¶ gerald_cleaver@baylor.edu

** qin_sheng@baylor.edu

¹ The hybrid approach [29–32] is quite similar to the dressed metric one, and the obtained results are observationally indistinguishable [33], so in this paper we do not consider it separately.

ics of the perturbations can be described by a quantum field propagating on a dressed background spacetime. On the other hand, the closed algebra approach requires no knowledge of underlying quantum theory. It's based on the effective constraints arising from the quantum corrections (either inverse triad or holonomy connections) and the requirement that effective constraint algebra be closed after the quantum corrections are taken into account. This anomaly-free condition helps fix the counter terms in the effective constraint and the resulting Poisson bracket of the scalar constraint with itself is deformed by a factor $\Omega(= 1 - 2\frac{\rho}{\rho_c})$, as compared to the classical case. The same factor is also present in the quantum equations of motion for cosmological perturbations and lies at the center of the problem called signature change [39, 40]². Finally, in the separate Universe approach, the cosmological spacetime with small perturbations is discretized into a lattice and loop quantization is applied to each cell which is assumed to be homogeneous and non-interacting with each other. In this way, the dynamics of cosmological perturbations can be approximated by the effective equations when the wave functions in each cell is sharply peaked. Although up to now only the scalar perturbations in the longitudinal gauge is quantized and the results are applicable only to the IR modes, it's the only one that performs loop quantization to both background and perturbations at the same time.

In the following, we will mainly focus on the closed algebra approach. Previous work [41–44] reveals the generic behavior of primordial power spectra in this approach, namely, scale invariance in the IR regime, oscillations for the intermediate scales and an exponential growth in the UV regime³. In particular, the exponential growth in the UV regime is due to the fact that the initial conditions are imposed in the contracting phase while the equations of motion for the cosmological perturbations become elliptic near the bounce point [41]. The divergence of power spectra in the UV regime is thought to be inconsistent with the observations as the observable window of the wave numbers in CMB is most probably located in this regime, considering the preferred number of inflationary e-folds is around 140 in LQC [42]. So far, there exist mainly two proposals to modify the UV behavior in this approach. The first one is to impose the initial conditions at the silent point so that the question of evolution of the mode function through the super-inflationary phase is avoided [46]. The second proposal is to address the trans-Planckian problem via the modified dispersion relations (MDRs) [47]. However, as the minimal non-zero length in LQG is still unknown due

to the complexity of the length operator, MDRs should be regarded as a phenomenological attempt towards solving the trans-Planckian problem in LQC.

In this paper, we will simply follow the first approach and choose the moment at which the initial conditions are imposed to be the silent point, so that the complications arising from the signature change near the bounce is circumvented. However, instead of imposing the initial conditions at the silent point, we flap the argument by asking what conditions are required at this moment, in order to produce predictions that are consistent with observations? To answer this question, we first present our analytical approximate solutions of the mode functions in the UV regime⁴, by applying the well-developed method, *the uniform asymptotic approximation (UAA) method*, which we have shown is very powerful in studying cosmological perturbations for various inflation models [18, 48–54]⁵. It is these analytical solutions that enable us to impose the observationally-consistent conditions at the end of inflation, and then evolve the mode functions backward until the silent point, whereby we read off the initial conditions at this silent point. Of course, this only tells us that if the initial conditions are chosen (at this silent point) in such a way, the resulted power spectra will be consistent with current cosmological observations. Clearly, the next question is what is the physics that leads to such conditions. Currently, we do not have a definite answer to it, and it is still under our investigations.

The paper is organized as follows. Sec. II is devoted to a concise review on the background evolution of the LQC Universe when the bounce is dominated by the kinetic energy of the scalar field. The pre-inflationary evolution of the scale factor and the scalar field is explicitly described by their analytical solutions of the Friedmann and Klein-Gordon equations. In Sec. III, with the UAA method, analytical solutions of the scalar mode function in the UV regime are derived. With the help of these analytical solutions, corrections to primordial power spectra due to the quantum gravitational effects at the Planck scale can now be parametrized in terms of the initial conditions imposed at the silent point. We then focus on finding a particular set of initial conditions that can produce results consistent with the observations. In this section, we also consider the IR regime[43]. In Sec. IV, similar analysis is carried out for the tensor perturbations. In particular, we first present the analytical solutions of the tensor modes in both UV and IR regimes, and then find the relation between the initial conditions at the silent point and the quantum corrections to the power spectra. Again, by requiring that the power spectrum at the end of inflation be the same as that obtained in general rela-

² Actually the existence of the signature change near the LQC bounce is still an open question, for more details, see the discussions in [38] and references therein.

³ In the dressed metric approach, the power spectra are enhanced and oscillating for the intermediate scales and scale-invariant in the UV regime [26, 45].

⁴ Recently, it was pointed out that the closed algebra approach might be applicable only to the infrared modes [38, 47].

⁵ All of the previous calculations of the power spectra in the UV regime rely on the numerical simulations.

tivity, we are able to identify a set of initial condition at the silent point. Finally, we summarize our main results and give some comments in Sec. V.

Throughout the paper, the Planck units are used in which $c = \hbar = G = 1$ so that the Planck length, time and mass are all equal to unity.

II. THE PRE-INFLATIONARY EVOLUTION IN LOOP QUANTUM COSMOLOGY

This section is mainly devoted to a review on the pre-inflationary evolution of the Universe in the spatially flat Friedmann-Lemaître-Robertson-Walker (FLRW) background described by

$$ds^2 = -dt^2 + a(t)dx_i dx^i, \quad (2.1)$$

where $a(t)$ is the cosmological scale factor and t is cosmic time. In LQC, the effective dynamics of a flat FLRW Universe is governed by the modified Friedmann equation [55, 56]

$$H^2 = \frac{8\pi}{3m_{\text{Pl}}^2} \rho \left(1 - \frac{\rho}{\rho_c}\right), \quad (2.2)$$

where $H \equiv \dot{a}/a$ denotes the Hubble parameter and dot represents the derivative with respect to the cosmic time, $m_{\text{Pl}}^2 = 1/G$ is the Planck mass, ρ is the energy density of the scalar field, and ρ_c is the critical energy density which represents the maximum value of the energy density in LQC and can be approximated by $\rho_c \simeq 0.41m_{\text{Pl}}^4$ [57]. In this paper, we only consider inflation sourced by a single scalar field. Therefore, in the matter sector, the effective equation of motion of the inflaton field with a potential $V(\phi)$ is just the Klein-Gordon equation given by

$$\ddot{\phi} + 3H\dot{\phi} + V_{,\phi} = 0, \quad (2.3)$$

where $V_{,\phi} \equiv dV(\phi)/d\phi$. As usual, the property of the scalar field can be well described by its effective equation of state ω_ϕ , which is defined via

$$\omega_\phi \equiv \frac{P}{\rho} = \frac{\frac{1}{2}\dot{\phi}^2 - V}{\frac{1}{2}\dot{\phi}^2 + V}, \quad (2.4)$$

where P represents the pressure of the scalar field.

A robust prediction of LQC is the occurrence of a non-singular quantum bounce, which removes the initial singularity in the deep Planckian regime purely due to the quantum geometric effects [10]. Eq. (2.2) shows that the quantum bounce occurs at $\rho = \rho_c$, where the energy density reaches its maximum value and the Hubble parameter becomes zero. The background evolution with a bouncing phase has been extensively studied [12–15], and one of the main results is that, right following the quantum bounce, a desired slow-roll inflation phase is attractive.

In the cosmological settings, it is also convenient to introduce the conformal time η via

$$\eta = \int_{t_{\text{end}}}^t \frac{dt'}{a(t')}, \quad (2.5)$$

so that at the end of the inflation $t = t_{\text{end}}$ and at the bounce time $t_B = 0$, the corresponding conformal times are given, respectively, by

$$\eta_{\text{end}} = 0, \quad \eta_B = \int_{t_{\text{end}}}^{t_B} \frac{dt'}{a(t')} < 0. \quad (2.6)$$

Moreover, previous studies on the background evolution in LQC with a chaotic potential also show that if the initial conditions are imposed in the remote past of the contracting phase, the most probable state at the bounce is dominated by the kinetic energy [13]. Furthermore, for the kinetic-energy-dominated bounce, a universal description of the background in the bouncing phase, irrespective of the specific form of the potential, is also known [18]. Thus, in this paper, we will concentrate on the background when the quantum bounce is dominated by the kinetic energy of the scalar field, in which it has been shown that the evolution of the universe between the quantum bounce and reheating can be universally divided into three different phases: *bouncing*, *transition* and *slow-roll inflation* [14–18]. In the rest part of this section, we will summarize the analytical solutions of the background evolution in these three phases.

A. The Bouncing Phase

The bouncing phase is characterized by the condition $\omega_\phi \approx 1$ for the kinetic dominated bounce. Therefore, the potential term in the evolution equations (2.2) and (2.3) can be ignored in the leading-order approximation. This results in two simplified equations

$$H^2 = \frac{4\pi G \dot{\phi}^2}{3} \left(1 - \frac{\dot{\phi}^2}{2\rho_c}\right), \quad (2.7)$$

$$\ddot{\phi} + 3H\dot{\phi} = 0, \quad (2.8)$$

where we have ignored the potential terms as $\dot{\phi}^2 \gg V(\phi)$ near the bounce. Then, from the Klein-Gordon equation (2.8), it's straightforward to obtain

$$\dot{\phi}(t) = \pm \sqrt{2\rho_c} \left(\frac{a(t)}{a_B}\right)^{-3}. \quad (2.9)$$

Here \pm correspond to the cases that $\dot{\phi}_B$ is positive or negative at the bounce, respectively. Substituting this into Eq. (2.7), we find

$$a(t) = a_B \left(1 + \frac{t^2}{\tau_B^2}\right)^{1/6}, \quad (2.10)$$

where $\tau_B = t_{\text{Pl}}/\sqrt{\gamma_B}$ and $\gamma_B \equiv \frac{24\pi\rho_c}{m_{\text{Pl}}^4} \approx 30.9$ is a dimensionless constant. From its definition in Eq. (2.5),

the conformal time η can be expressed in terms of the cosmic time as

$$\eta(t) - \eta_B = t {}_2F_1\left(\frac{1}{6}, \frac{1}{2}, \frac{3}{2}, -\frac{t^2}{\tau_B^2}\right), \quad (2.11)$$

where ${}_2F_1(a, b, c, z)$ is the hypergeometric function. Also using the analytical solution of $a(t)$ in Eq. (2.10), one finds that

$$\phi(t) = \phi_B \pm \frac{m_{\text{Pl}}}{2\sqrt{3}\pi} \operatorname{arcsinh}\left(\frac{t}{\tau_B}\right), \quad (2.12)$$

and

$$\dot{\phi}(t) = \pm \frac{\sqrt{2\rho_c}}{(1 + t^2/\tau_B^2)^{1/2}}. \quad (2.13)$$

B. The Transition Phase

This phase is characterized by a drastic drop of the equation of state ω_ϕ from positive to negative unity. Two particular moments are generally used to characterize this phase. The first one is denoted by t_c when the kinetic energy equals the potential energy, and at this moment, $\omega_\phi = 0$. The second is t_i at which ω_ϕ drops to negative one third which signifies the beginning of the acceleration of the Universe and thus can also be regarded as the beginning of the slow-roll inflation.⁶ As the transition phase is shortly-lived, lasting only less than one e-fold, it is quite reasonable to assume that the analytical solutions (2.10) and (2.12) from the bouncing phase remain valid until t_c . The validity of this assumption is checked in details in [18] with the chaotic and Starobinsky potentials, and the relative errors between the numerical and analytical solutions are shown to be less than 4%. Therefore, in this paper we directly employ (2.10) and (2.12) for the analytical approximations of the scale factor and scalar field during this phase, respectively.

C. The Inflationary Phase

During the slow-roll inflationary phase, the Universe is dominated by the potential energy of the scalar field and therefore experiencing an exponential expansion. The evolution of the scale factor can thus be approximated by

$$a(t) \approx a_i e^{H_{\text{inf}}(t-t_i)}, \quad (2.14)$$

here H_{inf} denotes the Hubble parameter in the slow-roll inflation and a_i is the scale factor at the onset of the slow-roll inflation whose explicit expression depends on

the form of the potential. Besides, the evolution of the scalar field is governed by the Klein-Gordon equation

$$3H\dot{\phi} + \frac{dV(\phi)}{d\phi} \approx 0. \quad (2.15)$$

Once the form of the potential is known, the solution ϕ can be found explicitly.

III. THE PRIMORDIAL SCALAR PERTURBATIONS

As the background evolution is known, it's appropriate to proceed to cosmological perturbations in LQC. In this section, we will focus on the scalar perturbations. First, the analytical approximations of the scalar mode functions will be given in both UV and IR regimes. Then, the relation between the initial conditions at the silent point and the power spectra in the UV regime will be fixed by matching the analytical solutions in the bouncing, transition and inflationary phases. Finally, we will discuss the possibility of choosing particular initial conditions that can produce primordial power spectra that are consistent with current observations.

A. The Mode Function and Co-moving Hubble Horizon

In the framework of the closed algebra approach, the mode function $\mu_S(\eta)$ for scalar perturbations obeys the equation [34–36]

$$\mu_S''(\eta) + \omega_k^2 \mu_S(\eta) = 0, \quad (3.1)$$

where

$$\omega_k^2 \equiv \Omega(\eta)k^2 - \frac{z_S''(\eta)}{z_S(\eta)}, \quad (3.2)$$

$$\Omega(\eta) \equiv 1 - \frac{2\rho(t)}{\rho_c}, \quad (3.3)$$

$$z_S(\eta) \equiv a \frac{\phi'}{\mathcal{H}} = a \frac{\dot{\phi}}{H}, \quad (3.4)$$

here k is the co-moving wavenumber, $\mathcal{H} \equiv a'/a$ and a prime denotes differentiation with respect to the conformal time η .

During the bouncing and transition phases, using the analytical approximations, namely, Eqs. (2.10) and (2.12), we find

$$\Omega(\eta) = \frac{\tau^2 - 1}{\tau^2 + 1}, \quad (3.5)$$

and

$$\frac{z_S''}{z_S} = \frac{\gamma_B (18 + 21\tau^2 - \tau^4)}{9\tau^2 (\tau^2 + 1)^{5/3}}, \quad (3.6)$$

⁶ To be precise, the acceleration of the Universe is not necessarily equivalent to the slow-roll inflation. However, once the Universe starts to accelerate, it quickly enters into the slow-roll inflation.

with $\tau \equiv t/\tau_B = t\sqrt{\gamma_B}$. In general, the qualitative evolution of the mode function μ_S depends on the sign of ω_k^2 . The modes with negative ω_k^2 are called decaying/growing modes, and these modes are outside the Hubble horizon. The modes with positive ω_k^2 are called oscillatory modes and they are inside the Hubble horizon. The complications in the closed algebra approach lie in the Ω factor of Eq. (3.2) which will change signs at $\rho = \frac{\rho_c}{2}$. The moment where $\Omega(\rho = \rho_c/2) = 0$ is called the silent point at which all the space points are de-correlated as the space-dependent term drops out from Eq. (3.1) and the two point functions on this surface become zero [46]. In the expanding phase, the silent point is always located at the end of the super-inflationary phase when $t = t_S \approx 0.18$. According to the signature of Ω , there are two distinctive regions: the Euclidean regime where Ω is negative and $\frac{\rho_c}{2} < \rho \leq \rho_c$; the Lorentzian regime where Ω is positive and $\rho < \frac{\rho_c}{2}$.

Taking into account the sign change of Ω across the silent point, the co-moving Hubble horizon (we will suppress the term ‘‘co-moving’’ in the following for simplicity) can be defined by

$$\lambda_S^2 = \Omega \frac{z_S}{z_S''}, \quad (3.7)$$

whose behavior in the post bounce phase is depicted in Fig. 1. At the bounce, the Hubble horizon equals zero as $z_S = 0$ at $t = t_B$. It remains negative during the super-inflationary phase from t_B to t_S . After t_S , the Hubble horizon continues to increase until $t = t_H$ when z_S'' equals zero and the Hubble horizon becomes infinitely large. In the interval $t_H < t < t_i$, the Hubble horizon is always negative which indicates all the relevant modes are now inside the horizon. Finally, t_i represents the onset of slow-roll inflationary phase in which the Hubble horizon decreases monotonically. The black dot-dashed horizontal line in Fig. 1 denotes a particular mode with co-moving number k . It's outside the horizon at the bounce point as Ω is negative near the bounce. At time $t = t_k$, this particular mode enters into the horizon and it remains inside the horizon until t_* when horizon crossing takes place during the slow-roll inflation. Although t_k and t_* do depend on the wavenumber of the particular mode, the generic behavior of scalar perturbations in the closed algebra is that all the modes experience horizon crossing twice in the post bounce phase. The first time is at point A indicating horizon-entry, and the second time is at point B indicating horizon-exit. As all the modes are outside the horizon at the bounce, the quantum effects near the bounce would affect all the modes from UV to IR regimes. This is different from the dressed metric approach in which there is a maximum wavenumber k_B , and the modes with wavenumber $k > k_B$ would not be affected by the dynamics around the bounce.

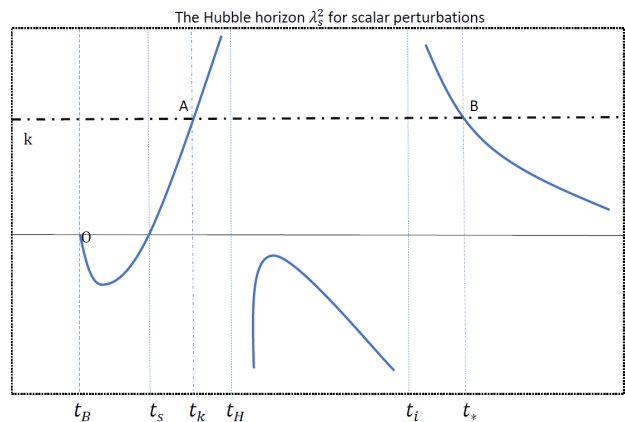


FIG. 1. A schematic plot of the Hubble horizon defined in Eq. (3.7). The solid curves show the evolution of the Hubble horizon λ_S^2 in the post bounce phase. t_B denotes the time at the bounce, t_S marks the moment when the super-inflationary phase is ended, $t_H \approx 0.84t_{P1}$ is the time when $z_S'' = 0$ and t_i is the time when the slow-roll inflation starts. The dot-dashed black line corresponds to the mode with co-moving wavenumber k which enters the horizon at t_k (point A) and later exits the horizon at t_* (point B) in the inflationary phase.

B. Uniform Asymptotic Approximation and Analytical Approximations of the Mode Function

In this subsection, we will give an outline of UAA in order to solve the mode function equation (3.1) (see [49] for a detailed exposition of the method for equations with one single turning point.). First, we need to put the mode equation into the standard form

$$\frac{d^2 \mu_S(y)}{dy^2} = \{g_S(y) + q(y)\} \mu_S(y), \quad (3.8)$$

where $y = -k\eta$ and

$$g_S(y) + q(y) = \frac{1 - \tau^2}{1 + \tau^2} + \frac{\gamma_B (18 + 21\tau^2 - \tau^4)}{9k^2\tau^2 (\tau^2 + 1)^{5/3}}. \quad (3.9)$$

At this point, use can be made of the Liouville transformation, which is

$$U(\xi) = \chi^{\frac{1}{4}} \mu_S(y) \quad \text{and} \quad \xi'^2 = \frac{|g_S|}{f^{(1)}(\xi)^2}, \quad (3.10)$$

where $\chi \equiv \xi'^2$, $\chi' = d\chi/dy$ and

$$f(\xi) = \int^y \sqrt{|g_S(y)|} dy, \quad f^{(1)}(\xi)^2 = \frac{df(\xi)}{d\xi}. \quad (3.11)$$

Consequently, the mode function equation (3.1) can now be transformed into

$$\frac{d^2 U}{d\xi^2} = [\pm f^{(1)}(\xi)^2 + \psi(\xi)] U, \quad (3.12)$$

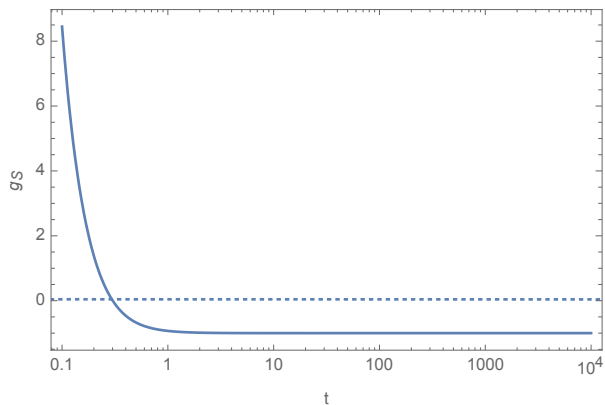


FIG. 2. This figure illustrates the general behavior of the function g_S . It shows explicitly that in the expanding phase when $t > 0$, g_S has only one turning point and it converges quickly to negative unity at large times. When plotting it, we had chosen $k = 5$.

where the \pm signs correspond to $g_S > 0$ and $g_S < 0$, respectively, and

$$\psi(\xi) = \frac{qt}{\chi} - \chi^{-3/4} \frac{d^2(\chi^{-1/4})}{dy^2}. \quad (3.13)$$

The key point in UAA is to find a proper choice of $q(y)$ and $f^{(1)}(\xi)^2$ so that the errors can be made as small as possible. To be concrete, in order to fix $q(y)$, one needs to first note that $g_S(y) + q(y)$ has a second-order pole at $t = 0$ (or equivalently $\eta = \eta_B$), that is

$$g_S(y) + q(y) \rightarrow \frac{2}{k^2 t^2} \quad \text{as } t \rightarrow 0^+. \quad (3.14)$$

According to the analysis of the error control function of UAA near the pole [54], one has to choose

$$q(y) = -\frac{1}{4k^2 t^2}, \quad (3.15)$$

for the convergence of error. So we have

$$g_S(y) = \frac{1 - \tau^2}{1 + \tau^2} + \frac{\gamma_B}{4k^2 \tau^2} + \frac{\gamma_B (18 + 21\tau^2 - \tau^4)}{9k^2 \tau^2 (\tau^2 + 1)^{5/3}}. \quad (3.16)$$

Thus, for an arbitrary mode (any fixed k), in the expanding phase, g_S is always a monotonically decreasing function of cosmic time as depicted in Fig. 2. Although the precise location of the turning point t_+ , namely $g_S(t_+) = 0$, does depend on the co-moving wavenumber k , qualitative behavior of g_S remains the same for all the modes, that is, g_S has only one turning point in the bouncing and transition phases for any given k .

Once the property of g_S is known, we can make a good choice of $f^{(1)}(\xi)^2$. Generally, the choice of $f^{(1)}(\xi)^2$ relies on the properties of the turning points of g_S which, as

discussed above, has only one single turning point in the expanding phase. As a result, one can simply choose

$$f^{(1)}(\xi)^2 = \pm \xi, \quad (3.17)$$

again the \pm signs are assigned, respectively, in the regions where g_S is positive/negative. Now that $q(y)$ and $f^{(1)}(\xi)^2$ are fixed, the leading-order approximation of the mode function can be derived by simply ignoring the $\psi(\xi)$ term in Eq. (3.12), which leads to

$$\mu_S(t) = \left(\frac{\xi_S}{g_S} \right)^{1/4} \left\{ a_k \text{Ai}(\xi_S) + b_k \text{Bi}(\xi_S) \right\}, \quad (3.18)$$

where a_k, b_k are two integration constants, A_i and B_i are the Airy functions of the first and second kind, respectively. Besides, ξ_S is given explicitly by the integral

$$\xi_S = \begin{cases} \left(-\frac{3k}{2} \int_{t_+}^t \frac{\sqrt{g_S}}{a(t)} dt \right)^{2/3}, & t < t_+ \\ -\left(\frac{3k}{2} \int_{t_+}^t \frac{\sqrt{-g_S}}{a(t)} dt \right)^{2/3}, & t > t_+. \end{cases} \quad (3.19)$$

Moreover, the mode function $\mu_S(t)$ satisfy the Wronskian condition

$$\mu_S \dot{\mu}_S^* - \mu_S^* \dot{\mu}_S = \frac{i}{a(t)}, \quad (3.20)$$

where a dot denotes the derivative with respect to the cosmic time. In terms of the integration constants, the Wronskian condition takes the form

$$a_k b_k^* - a_k^* b_k = \frac{i\pi}{k}. \quad (3.21)$$

It should be noted that the validity of our analytical approximations (3.18) is justified only when the discarded term ψ is relatively small compared with ξ . Our simulations show this is indeed the case if $k \geq 1$. In Fig. 3, we choose $k = 5$ and compare the analytical solution with the numerical one. As ψ is less than one percentage of ξ in the bouncing and transition phases, our analytical approximations are in a good match with the numeric one.

C. Primordial Power Spectrum in the UV Regime

The observable window of wave numbers in the current CMB observations ranges between $k_{\min} = 10^{-4} \text{Mpc}^{-1}$ and $k_{\max} = 1 \text{Mpc}^{-1}$.⁷ In LQC, at the bounce, there is a characteristic energy scale given by

$$k_B \equiv a_B \sqrt{\rho_c} M_{\text{Pl}}^{-1}. \quad (3.22)$$

The modes with $k \gg k_B$ are located in the ultraviolet (UV) regime while modes with $k \ll k_B$ are in the infrared (IR) regime, and modes with $k \approx k_B$ are in the

⁷ $\text{Mpc}^{-1} \approx 5.24 \times 10^{-58}$ in the Planck units.

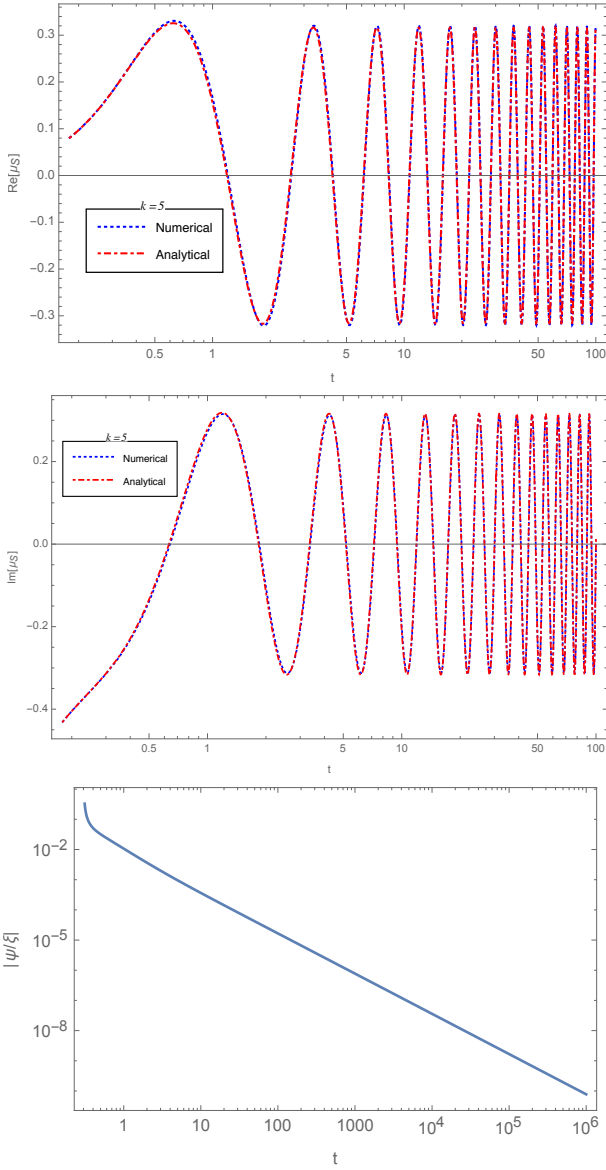


FIG. 3. In this figure, we compare the numerical solution (red) of Eq. (3.1) with our analytical one (blue) in Eq. (3.18) for $k = 5$. Initial conditions are imposed at the silent point by setting $a_k = ib_k = \sqrt{\frac{\pi}{2k}}$. The first two subfigures show the difference in the real and imaginary parts of analytical and numerical solutions. In the last subfigure, we show the comparative magnitude between ψ and ξ which explains why our approximations are in a good fit with the numeric solution.

intermediate regime. As the physical lengths of the primordial perturbations are stretched out in an expanding Universe, it's important to determine which range of the observable window at the present corresponds to at the bounce. Generally, the answer to this question depends on the history of the Universe since

$$k_{\text{phy}}^B = e^N k_{\text{phy}}, \quad (3.23)$$

where k_{phy}^B represents the physical length of the mode at the bounce and k_{phy} is the physical length at the present, N denotes the total e-foldings from the bounce to the present. Previous investigations [13, 18] on the pre-inflationary dynamics in LQC indicate that the preferable e-foldings from the bounce to the end of inflation is around $N_{\text{inf}} = 140$ which gives a rough estimate on the total e-foldings $N \approx 200$. This implies that the modes with the longest wavelength that can be observed today was located in the deep UV regime at the bounce, $k_{\text{min}}^B \sim 10^{25}$. Of course, by fine-tuning the initial conditions in the contracting phase (or at the bounce), the observable window can also be moved to the IR regime. The minimal requirement is $k_{\text{max}}^B \approx 1$ which implies the e-foldings from the bounce to the end of inflation should be around $N_{\text{inf}} \approx 70$.

In the UV regime, $k \gg 1$, the analytical approximations of the turning point, scalar mode function and primordial power spectrum can be derived order by order in terms of the Taylor expansion of the inverse wavenumber. Specially, when near the silent point, the turning point can be expanded into the series

$$t_+^{\text{UV}} = t_S + \frac{\delta_S^{\text{UV}}}{k^2} + \mathcal{O}\left(\frac{1}{k^3}\right), \quad (3.24)$$

where $t_S = \frac{1}{\sqrt{\gamma_B}}$ and $\delta_S^{\text{UV}} = \sqrt{\gamma_B} \left(\frac{1}{4} + \frac{19 \times 2^{1/3}}{18}\right)$. Consequently,

$$\xi_S(t_S) \approx \left(\frac{3\sqrt{g(t_S)}\delta_S^{\text{UV}}}{2ka(t_S)}\right)^{2/3} = \xi_S^{\text{UV}} k^{-4/3}, \quad (3.25)$$

where $\xi_S^{\text{UV}} = \frac{(9+38 \times 2^{1/3})\gamma^{2/3}}{12 \times 2^{7/9} \times 3^{1/3}} \approx 0.735$. In the above approximation, only the leading-order term is retained. Now, it's straightforward to compute the power spectrum at the silent point, which is

$$\begin{aligned} \Delta_{\mathcal{R}}^2(t_S) &= \lim_{\tau \rightarrow 1} \frac{k^3}{2\pi^2} \left| \frac{\mu_S}{z_S} \right|^2 \\ &\approx \Delta_S^{\text{UV}} k^{10/3} \left\{ |a_k|^2 A_S^2 + |b_k|^2 B_S^2 \right. \\ &\quad \left. + a_k^* b_k A_S B_S + a_k b_k^* A_S B_S \right\}, \end{aligned} \quad (3.26)$$

where $\Delta_S^{\text{UV}} \equiv \frac{3^{1/3} \gamma_B^{5/6}}{72 \times 2^{13/18} \pi^2 \rho_c}$ and $B_S^2 = 3A_S^2 = 3^{-1/3} \Gamma^{-2}(2/3)$.

In the transition phase when $t \approx 10^4 \sim 10^5$, $\xi_S(t)$ approaches asymptotically to negative infinity, and in this asymptotic region, owing to the asymptotic forms of the Airy functions,

$$\text{Ai}(\xi) \rightarrow \frac{1}{\sqrt{\pi(-\xi)^{1/4}}} \cos\left[\frac{2}{3}(-\xi)^{3/2} - \frac{\pi}{4}\right], \quad (3.27)$$

$$\text{Bi}(\xi) \rightarrow -\frac{1}{\sqrt{\pi(-\xi)^{1/4}}} \sin\left[\frac{2}{3}(-\xi)^{3/2} - \frac{\pi}{4}\right]. \quad (3.28)$$

Then, the mode function takes the form

$$\mu_S = \frac{1}{\sqrt{\pi(-g)^{1/4}}} \left\{ a_k \cos\left[\frac{2}{3}(-\xi)^{3/2} - \frac{\pi}{4}\right] \right.$$

$$+b_k \sin \left[\frac{2}{3}(-\xi)^{3/2} - \frac{\pi}{4} \right] \}. \quad (3.29)$$

On the other hand, in the transition phase, as the Hubble horizon approaches to the negative infinity as shown in Fig. 1, the mode function equation (3.1) simply reduces to

$$\mu_S'' + k^2 \mu_S = 0, \quad (3.30)$$

which has the solution

$$\mu_S = \frac{1}{\sqrt{2k}} \left(\tilde{\alpha}_k e^{-ik\eta} + \tilde{\beta}_k e^{ik\eta} \right), \quad (3.31)$$

where $\tilde{\alpha}_k$ and $\tilde{\beta}_k$ are two parameters whose explicit expressions can be found from Eq. (3.29) in the following way. In the UAA, by definition,

$$\frac{2}{3}(-\xi)^{3/2} = k \int_{\eta_+}^{\eta} \sqrt{-g_S(\eta)} d\eta. \quad (3.32)$$

Noting that $g_S(\eta) = g_S(t)$ quickly converges to the negative unity as depicted in Fig. 2, we can therefore assume that after $\eta = \eta_f$, the function $g_S(\eta) \simeq -1$. Therefore,

$$\begin{aligned} \frac{2}{3}(-\xi)^{3/2} &= k \int_{\eta_+}^{\eta} \sqrt{-g_S(\eta)} d\eta \\ &= k\eta - k\eta_f + k \int_{\eta_+}^{\eta_f} \sqrt{-g_S(\eta)} d\eta. \end{aligned} \quad (3.33)$$

Defining

$$\begin{aligned} \eta_{fB} &= \eta_f - \int_{\eta_+}^{\eta_f} \sqrt{-g_S(\eta)} d\eta, \\ &= \eta_B + \hat{\eta}(t_f), \end{aligned} \quad (3.34)$$

where $\hat{\eta}(t)$ is defined by

$$\hat{\eta}(t) = t {}_2F_1 \left(\frac{1}{6}, \frac{1}{2}, \frac{3}{2}, -\frac{t^2}{\tau_B^2} \right) - \int_{t_+}^t \frac{\sqrt{-g_S(t)} dt}{a(t)}. \quad (3.35)$$

Now, Eq. (3.29) can be written into

$$\begin{aligned} \mu_S &= \frac{e^{-i\pi/4}}{2\sqrt{\pi}} \left\{ (a_k - ib_k) e^{ik(\eta - \eta_{fB})} \right. \\ &\quad \left. + (ia_k - b_k) e^{-ik(\eta - \eta_{fB})} \right\}, \end{aligned} \quad (3.36)$$

which, once compared with Eq. (3.31), leads to the connections between the two sets of integration constants, given by

$$\tilde{\alpha}_k = \sqrt{\frac{k}{2\pi}} (ia_k - b_k) e^{ik\eta_{fB} - i\pi/4}, \quad (3.37)$$

$$\tilde{\beta}_k = \sqrt{\frac{k}{2\pi}} (a_k - ib_k) e^{-ik\eta_{fB} - i\pi/4}, \quad (3.38)$$

with the Wronskian condition $|\tilde{\alpha}|^2 - |\tilde{\beta}|^2 = 1$.

Right after the transition phase, when the energy density drops to about $10^{-12} \rho_c$, the slow-roll inflation takes

place. During this phase, the mode functions can be expanded in terms of the Hankel functions. An analysis on the mode function [18] reveals that the power spectrum in this phase can be computed by the formula

$$\Delta_{\mathcal{R}}^2 = |\alpha_k + \beta_k|^2 \Delta_{\mathcal{R}}^{\mathcal{GR}}, \quad (3.39)$$

where $\alpha_k = \tilde{\alpha}_k$, $\beta_k = \tilde{\beta}_k$ and the power spectrum in the classical theory $\Delta_{\mathcal{R}}^{\mathcal{GR}}$ is given by

$$\Delta_{\mathcal{R}}^{\mathcal{GR}} \equiv \frac{k^2}{2\pi^3} \left(\frac{H}{a\dot{\phi}} \right)^2 \Gamma^2(\nu_s) \left(\frac{-k\eta}{2} \right)^{1-2\nu_s}, \quad (3.40)$$

with $\nu_s^2 \approx \eta^2 z_S''/z_S + 1/4$. In general, the power spectrum for a particular mode is computed at the horizon crossing when $k_* = a(t_*)H(t_*)$ as all the modes are frozen outside the horizon. Besides, in Eq. (3.39), the corrections due to the quantum gravitational effects near the bounce are parametrized by the coefficients α_k and β_k which in turn can be directly related to the initial conditions at the silent point, if Eqs. (3.37)-(3.38) are taken into account. It can be shown easily that the averaged power spectrum is related to the classical result via

$$|\alpha_k + \beta_k|^2 = \frac{k}{\pi} (|a_k|^2 + |b_k|^2). \quad (3.41)$$

Therefore, if we require the quantum corrections are negligible, namely, $\mathcal{P}_{\mathcal{R}} = \mathcal{P}_{\mathcal{R}}^{\mathcal{GR}}$, then the condition on the initial data at the silent point should be

$$|a_k|^2 + |b_k|^2 = \frac{\pi}{k}. \quad (3.42)$$

The only initial data that satisfy both Eq. (3.42) and the Wronskian condition (3.21) is

$$a_k = \sqrt{\frac{\pi}{2k}}, \quad b_k = -i\sqrt{\frac{\pi}{2k}}, \quad (3.43)$$

which fix the form of initial power spectrum at the silent point to be

$$\Delta_{\mathcal{R}}^2 \propto k^{\frac{7}{3}}. \quad (3.44)$$

Moreover, if the initial condition (3.43) is substituted back into Eq. (3.36), one can immediately find that during the transition phase, the Universe is in the BD vacuum. This explains why (3.43) can lead to the classical results.

To confirm this point, the numeric simulations of the power spectrum are presented in Fig. 4. In the top panel, the initial condition (3.43) at the silent surface are used. It can be seen from the graph that although the power spectrum is oscillating at large wavenumbers ($k > 1$), its average value is scale-invariant and its order of magnitude is also as expected ($\approx 2.2 \times 10^{-9}$) from 2015 Planck data. We also try several different sets of initial conditions, and all give a divergent behavior, as shown by the bottom panel of Fig. 4, which is consistent with the numerical

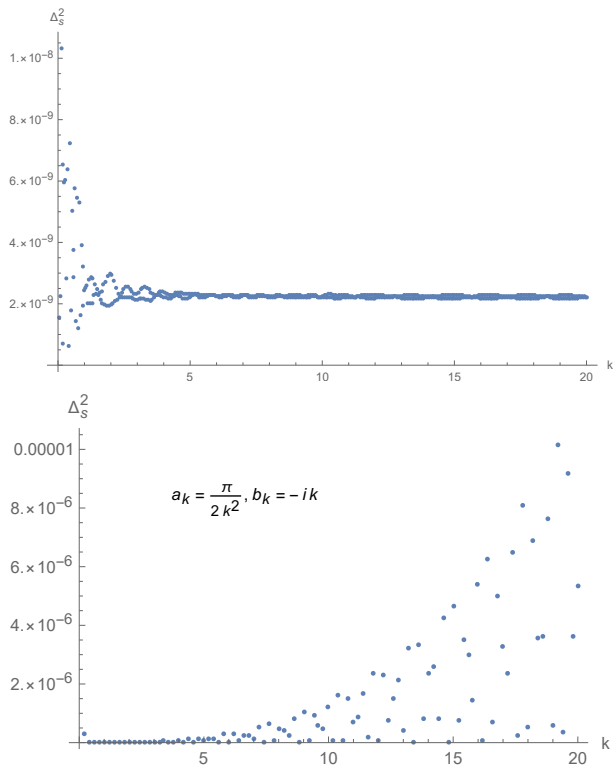


FIG. 4. Primordial power spectrum for the scalar perturbations when the Universe is filled with a single scalar field with the chaotic potential. The mass of the scalar field is chosen to be 1.26×10^{-6} and the initial condition for the background evolution is set at the bounce with $\phi_B = 5.6$ and $\dot{\phi} < 0$. The top panel is the power spectrum resulting from the initial condition (3.43) which leads to a scale-invariant power spectrum at large wavenumbers, while the bottom panel corresponds to the initial condition(3.45).

results obtained previously [42, 47]. Note that in plotting the bottom panel of Fig. 4, we have chosen

$$a_k = \frac{\pi}{2k^2}, \quad b_k = -ik, \quad (3.45)$$

at the silent surface.

To conclude this section, we would like to show that the initial condition (3.43) is in fact the only one that will generate the primordial power spectrum equal to the classical result in the observable regime, and other choices of the initial conditions will inevitably lead to a correction term proportional to some positive power of the co-moving wavenumber, and hence a divergent power spectrum in the UV regime. In order to prove this, one can start with a more general parameterization

$$a_k = a_0 k^n, \quad b_k = b_0 e^{-i\theta} k^l, \quad (3.46)$$

where θ is the relative phase between a_k and b_k . Besides, both a_0 and b_0 are positive and independent of k . With these new parameters, the Wronskian condition is now equivalent to

$$2a_0 b_0 \sin \theta = \pi, \quad n + l = -1. \quad (3.47)$$

Thus, the quantum corrections can now be written as

$$|\alpha_k + \beta_k|^2 = \frac{1}{\pi} (a_0^2 k^{2n+1} + b_0^2 k^{-2n-1}). \quad (3.48)$$

Combining Eqs. (3.47) and (3.48), one can immediately conclude

$$|\alpha_k + \beta_k|^2 = 1 \iff n = l = -\frac{1}{2}, \quad \sin \theta = 1. \quad (3.49)$$

D. Primordial Power Spectrum in the IR Regime

The calculations of the power spectrum in the IR regime has already been discussed in great details in [43]. Although, in their paper, the initial conditions are chosen in the remote past of the contracting phase, the results are actually independent of the time (up to a rescaling of the power spectrum), once the initial conditions are chosen. The reason is as follows. In the IR regime as $k \ll 1$, throughout its evolution in the bouncing and transition phases, the mode function equation (3.1) has the approximate solution

$$\mu_S = a_k z_S + b_k z_S \int_{\eta_*}^{\eta} \frac{d\eta'}{z_S^2} + \mathcal{O}(k^2), \quad (3.50)$$

where η_* denotes some particular time. As a result, the power spectrum at any time is given by

$$\begin{aligned} \Delta_S^{\text{IR}}(\eta) &= \frac{k^3}{2\pi^2} \left| \frac{\mu_S}{z_S} \right|^2, \\ &= \frac{k^3}{2\pi^2} \left| a_k + b_k \int_{\eta_*}^{\eta} \frac{d\eta'}{z_S^2} \right|^2. \end{aligned} \quad (3.51)$$

In general, the power spectrum can be obtained by evaluating the integral in Eq. (3.51) explicitly at the end of the slow-roll inflation $\eta = \eta_{\text{end}}$. Here, the key observation is that the integral $\int_{\eta_*}^{\eta_{\text{end}}} d\eta' / z_S^2$ turns out to be only dependent on the background dynamics and therefore irrespective of any particular mode. All the information concerning the wavenumber k is incorporated into the integration constants a_k and b_k which satisfy the Wronskian condition

$$a_k b_k^* - a_k^* b_k = i. \quad (3.52)$$

With the parameterization (3.46), the above Wronskian condition is equivalent to

$$2a_0 b_0 \sin \theta = 1, \quad n + l = 0. \quad (3.53)$$

Thus, the only set of initial conditions that can lead to a scale-invariant power spectrum is the one chosen in [43], namely $l = -n = -3/2$, so that

$$a_k \propto k^{3/2}, \quad b_k \propto k^{-3/2}. \quad (3.54)$$

With such a choice, the power spectrum turns out to be scale-invariant at any given time from the bouncing phase to the end of slow-roll inflation.

IV. THE PRIMORDIAL TENSOR PERTURBATIONS

The analysis of tensor perturbations in closed algebra approach can be carried out in the same way as the scalar perturbations given in the last section. The only complications come from the fact that the tensor mode function becomes divergent at the silent point. However, with the analytical approximations from UAA, we can easily regularize the divergence. Finally, a finite power spectrum at the silent point is found and an explicit relation between the initial conditions at the silent point and the resulting power spectrum is given.

A. The Mode Function and Co-moving Hubble Horizon

The equation of motion for the primordial tensor perturbations takes the form [34–36]

$$\mu_T''(\eta) + \left[\Omega(\eta)k^2 - \frac{z_T''}{z_T} \right] \mu_T(\eta) = 0, \quad (4.1)$$

where $\Omega(\eta)$ is defined in Eq. (3.5) and

$$z_T(\eta) = \frac{a(\eta)}{\sqrt{\Omega(\eta)}}. \quad (4.2)$$

It should be noted that unlike z_S in the scalar perturbations, z_T is singular at the silent point, which leads to the mode function singular at the silent point, too. The background evolution is still described by Eqs. (2.10) and (2.12). Analogous to the Hubble horizon (3.7) in Sec. III, we can also define the Hubble horizon of the tensor perturbations via

$$\lambda_T^2 = \Omega \frac{z_T''}{z_T}. \quad (4.3)$$

As shown in Fig. 5, the qualitative behavior of the Hubble horizon in the tensor perturbations is analogous to the scalar ones. The only quantitative difference occurs at the bounce. In the scalar perturbation, $\lambda_S^2(t_B) = 0$ while in tensor perturbations, $\lambda_T^2(t_B) \approx -0.014$. As a result, all the analysis given in Sec. III. A on the Hubble horizon can also apply to the tensor case. In particular, all the modes are initially outside the horizon at the bounce and later enter the horizon at a time that is in the interval $t_S < t < t_H$. Afterwards, these modes remain inside the horizon when $t_H < t < t_i$ and then exit the horizon during the slow-roll inflation.

In order to find analytical solutions, we first write Eq. (4.1) in the standard form with the new argument $y = -k\eta$,

$$\frac{d^2 \mu_T(y)}{dy^2} = \left\{ g_T(y) + q_T(y) \right\} \mu_T(y), \quad (4.4)$$

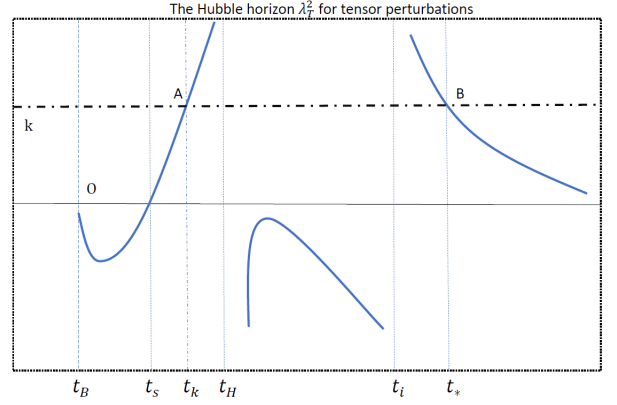


FIG. 5. A schematic plot of the Hubble horizon in the tensor perturbation. In the figure, the solid curves depict the behavior of the Hubble horizon λ_T^2 in the pre-inflationary phase. t_B denotes the bounce time, t_S is the time when the super-inflationary phase ends, $t_H \approx 0.91t_{P1}$ is the time when $z_T'' = 0$ and t_i again signifies the onset of the slow-roll inflation. At the bounce, $\lambda_T^2(t_B) = -0.014$. A particular mode with co-moving wavenumber k is also marked out. It enters the horizon at point A when $t = t_k$ and exits it in the inflationary phase at point B when $t = t_*$.

where

$$g_T(y) + q_T(y) = \frac{(1 - \tau^2)}{1 + \tau^2} + \frac{\gamma_B (21 + 47\tau^2 + 41\tau^4 - \tau^6)}{9k^2 (\tau^2 - 1)^2 (\tau^2 + 1)^{5/3}}, \quad (4.5)$$

which has a pole located at the silent point $\tau^2 = 1$ since

$$g_T(y) + q_T(y) \rightarrow \frac{3\sqrt{54}\gamma_B}{k^2 (\tau^2 - 1)^2}. \quad (4.6)$$

Following the analysis of the error control function, for a second-order pole, one has to choose [54]

$$q_T(y) = -\frac{2^{1/3}\gamma_B}{k^2(1 - \gamma_B t^2)^2}, \quad (4.7)$$

which leads to

$$g_T(y) = \frac{(1 - \tau^2)}{1 + \tau^2} + \frac{2^{1/3}\gamma_B}{k^2 (\tau^2 - 1)^2} + \frac{\gamma_B (21 + 47\tau^2 + 41\tau^4 - \tau^6)}{9k^2 (\tau^2 - 1)^2 (\tau^2 + 1)^{5/3}}. \quad (4.8)$$

The behavior of g_T is analogous to g_S presented in Sec. II.B, that is, g_T has only one single turning point in the bouncing and transition phases and also quickly converges to the negative unity. Consequently, all the formulae in Sec. II.B for the scalar modes are also applicable to the tensor modes as long as g_S is replaced by g_T given in Eq. (4.8). In particular, the analytical solution of the tensor modes is given by

$$\mu_T = \left(\frac{\xi_T}{g_T} \right)^{1/4} \left\{ a_k \text{Ai}(\xi_T) + b_k \text{Bi}(\xi_T) \right\}, \quad (4.9)$$

with

$$\xi_T = \begin{cases} \left(-\frac{3k}{2} \int_{t_+}^t \frac{\sqrt{g_T(t)}}{a(t)} dt \right)^{2/3}, & t < t_+ \\ -\left(\frac{3k}{2} \int_{t_+}^t \frac{\sqrt{-g_T(t)}}{a(t)} dt \right)^{2/3}, & t > t_+, \end{cases} \quad (4.10)$$

where t_+ represents the turning point of g_T , i.e. $g_T(t_+) = 0$. In Fig. 6, we compare the analytical solution with the numerical one for $k = 10$. As the mode function becomes divergent at the silent point, the initial conditions are chosen at $t = 5$ with $a_k = ib_k = \sqrt{\frac{\pi}{2k}}$. The smallness of the ratio ψ/ξ_T in the last subfigure indicates Eq. (4.9) is a good approximation in the bouncing and transition phases. We have also checked our solution in the UV regime for $k > 1$, and found that our analytical approximations are valid and fit with the numeric ones very well. However, in the IR regime, as ψ becomes the same order of ξ , higher-order corrections need to be taken into account.

B. Primordial Power Spectrum

In this section, we will consider the asymptotic forms of our analytical solutions in both of the UV and IR regimes, although we will pay more attention in the UV regime.

In the limit $k \gg 1$, the turning point t_+ has the following expansion

$$t_+ = \frac{1}{\sqrt{\gamma_B}} + \frac{\delta_1}{k^{2/3}} + \mathcal{O}\left(\frac{1}{k^{4/3}}\right), \quad (4.11)$$

which, once plugged into Eq. (4.8), yields $\delta_1 = \frac{2^{1/9}}{\gamma_B^{1/6}} \approx 0.61$. As δ_1 is a positive number, the relation $t_+ > t_S$ always holds in the UV regime. Therefore, only the upper branch of Eq. (4.10) is required. To regularize its divergence at the silent point, we can define

$$\xi_T(t_S) \equiv \lim_{\epsilon \rightarrow 0} \xi_T(t_S + \epsilon). \quad (4.12)$$

From the Taylor expansion of the integrand of Eq. (4.10)

$$\frac{\sqrt{g_T(t)}}{a(t)} = \frac{1}{k(t - t_S)} - \frac{5\sqrt{\gamma_B}}{12k} + \mathcal{O}(\epsilon), \quad (4.13)$$

we find that ξ_T around the silent point can be shown as

$$\xi_T(t_S + \epsilon) = \left[\frac{3}{2} \ln\left(\frac{\delta_1}{k^{2/3}}\right) - \frac{3}{2} \ln \epsilon + \mathcal{O}(\epsilon) \right]^{2/3}. \quad (4.14)$$

Thus, it becomes obvious that as ϵ tends to zero, ξ_T goes to positive infinity and consequently the mode function becomes divergent at the silent point. By virtue of the asymptotic forms of the Airy functions,

$$\text{Ai}(\xi_T) \rightarrow \frac{e^{-\frac{2}{3}\xi_T^{3/2}}}{2\sqrt{\pi}\xi_T^{1/4}}, \quad \text{Bi}(\xi_T) \rightarrow \frac{e^{\frac{2}{3}\xi_T^{3/2}}}{\sqrt{\pi}\xi_T^{1/4}}, \quad (4.15)$$

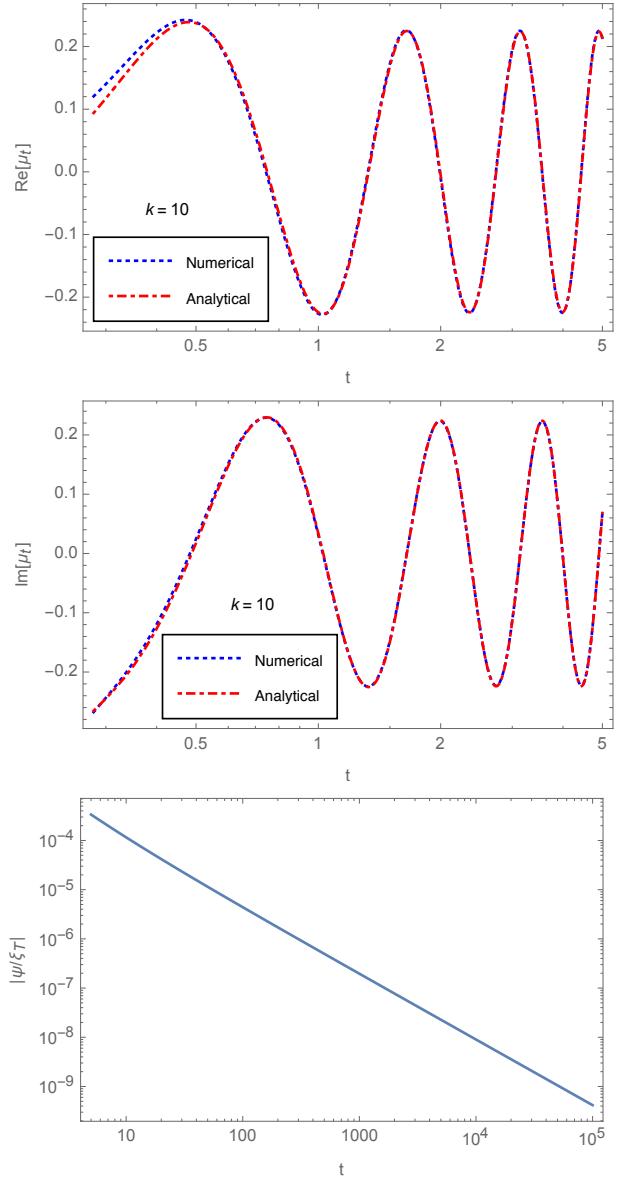


FIG. 6. In this figure, approximate solutions (4.9) (red) are compared with the numerical one (blue) by choosing the initial conditions at the time $t = 5$ with $a_k = ib_k = \sqrt{\pi/2k}$. In the last subfigure, the ratio ψ/ξ_T is depicted until the transition phase $t = 10^5$.

as $\xi_T \rightarrow +\infty$, it's straightforward to show that

$$\begin{aligned} \mu_T(t_S) &= \lim_{\epsilon \rightarrow 0} \frac{b_k e^{\frac{2}{3}\xi_T^{3/2}}}{g_T^{1/4} \sqrt{\pi}}, \\ &= \lim_{\epsilon \rightarrow 0} \frac{b_k \delta_2 k^{-1/6} \epsilon^{-1/2}}{\sqrt{\pi}}, \end{aligned} \quad (4.16)$$

with $\delta_2 = \left(\frac{2}{\gamma_B}\right)^{\frac{1}{36}}$. Now the power spectrum at the silent

point can be computed as

$$\begin{aligned}\Delta_t^2(t_S) &\equiv \lim_{t \rightarrow t_S} \frac{32k^3}{\pi} \left| \frac{\mu_T}{z_T} \right|^2, \\ &= \frac{2^{\frac{83}{18}} |b_k|^2 \gamma_B^{\frac{1}{6}} k^{\frac{8}{3}}}{\pi^2}.\end{aligned}\quad (4.17)$$

It's interesting to observe that even though our analytical mode function (4.16) becomes divergent at the silent point, the resulting power spectrum (4.17) is still finite. Besides, it only depends on the magnitude of parameter b_k of the mode function. The effects of a_k simply dies away as $t \rightarrow t_S$. Following the same line of arguments in Sec. II, if we require that the quantum corrections be negligible, the only possible initial conditions at the silent point are given by Eq. (3.43) which in turns fix the initial power spectrum to be

$$\Delta_t^2(t_S) \propto k^{\frac{5}{3}}. \quad (4.18)$$

All the other choices of the initial conditions will result in power spectra that become divergent in the UV limit, and hence are inconsistent with observations. In Fig. 7, the numeric simulations of the power spectrum for the tensor modes are presented with the initial conditions (3.43) (top panel) and ($a_k = \frac{\pi}{2k^2}, b_k = -ik$) (bottom panel). With the initial condition (3.43), the averaged power spectrum at large wavenumber become scale-invariant and its magnitude is around 3.3×10^{-10} , while the numeric simulations with a_k and b_k given by Eq.(3.45) at the silent surface display a divergent behavior of the power spectrum at large k . As a matter of fact, the initial condition (3.43) is the only one that leads to a power spectrum that is consistent with current observations. The proof is quite similar to the scalar case, and we shall not repeat it here.

The calculations of the tensor power spectrum in the IR regime proceeds in the same way as for the scalar perturbations. All the formulae in Sec. III. D are still valid here as long as z_S in Eqs. (3.50) and (3.51) is replaced by z_T . Then, it can be shown that, in order to produce a scale-invariant power spectrum in the IR regime, the only possible choice of n and l is still $l = -n = 3/2$. Such resulted power spectrum in fact is scale-invariant not only at the silent point but also at any given time in the bouncing, transition and inflationary phases.

V. SUMMARY

In this work, using the uniform asymptotic approximations (UAA), we have explicitly derived the analytical solutions of both scalar and tensor mode functions in the closed algebra approach in LQC. We have also discussed the co-moving Hubble horizon when the bounce is dominated by the kinetic energy of the scalar field and found all the modes are outside the Hubble horizon at the silent point ($\approx 0.18t_{P1}$). Shortly after the super-inflationary phase, all these modes enter the Hubble

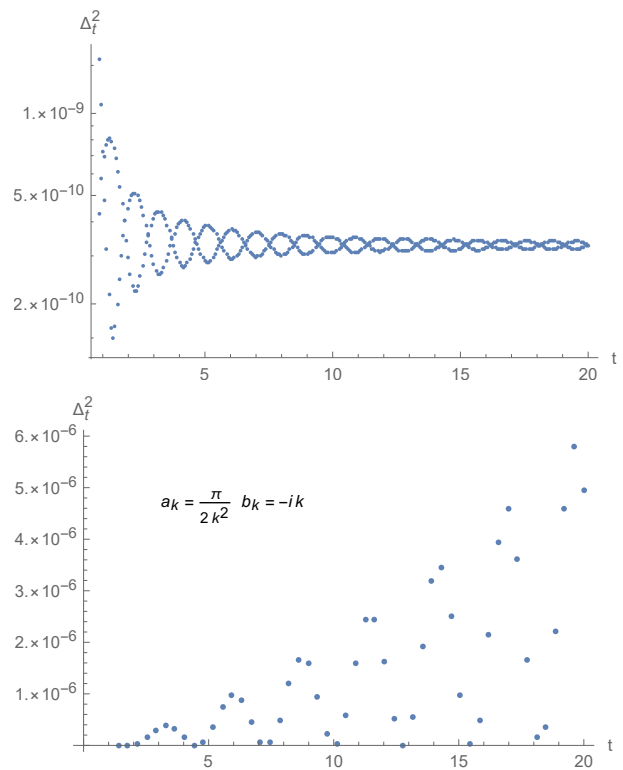


FIG. 7. Primordial power spectrum for the tensor modes when the Universe is filled with a single scalar field with the chaotic potential. The mass of the scalar field and the initial conditions for the background evolution are the same as in Fig. 4. The top panel is the result from the initial condition (3.43), while in the bottom panel, the initial conditions are set to (3.45) at the silent surface.

horizon at about t_{P1} and then re-exit the horizon during the slow-roll inflationary phase. In order to avoid the problem caused by the signature change in the super-inflationary phase, our initial conditions are chosen to be imposed at the silent point. Matching the solutions in the bouncing, transition and inflationary phases, we have shown how the quantum corrections are related to the initial conditions at the silent point for both scalar and tensor perturbations.

Although previous numerical simulations show a divergent behavior of the power spectra in the UV regime, we have found a particular set of initial conditions at the silent point [cf. Eq. (3.43)], which can reproduce results that are consistent with current observations. In doing so, it turns out that the initial power spectra also depend on the wavenumber as shown in Eqs. (3.44) and (4.18) for the scalar and tensor perturbations, respectively. All the other choices of the initial conditions (at the silent point) would inevitably lead to divergent power spectra in the UV regime. On the other hand, the calculations in the IR regime are based on the fact that there exist analytical solutions of the mode function equations when the term Ωk^2 is ignored. It turns out that the initial conditions at the silent point completely determines the k -dependence

of the power spectra in the IR regime. More specifically, the scale-invariant properties of the power spectra in the IR regime demands the conditions (3.54) to be satisfied. This choice is equivalent to the Bunch-Davies vacuum in the contracting phase and it will result in scale-invariant power spectra at any given time in the bouncing, transition and inflationary phases.

Finally, we would like to emphasize that in this work, we have applied UAA to the equations of motion for cosmological perturbations originally proposed in [36] and assumed that they are valid for all modes. However, as argued in [38], the deformed algebra approach is valid only in the regime where the dynamics can be well approximated by the effective equations. This indicates the large quantum fluctuations are ruled out in this approach

from the beginning. As a result, the closed algebra approach is only applicable to the long-wavelength modes. Then, in order to modify the UV behavior, it's essential to add quantum corrections to account for the UV modes. One of the tentative approaches is MDRs discussed in [47]. We wish to come to this issue in another occasion.

VI. ACKNOWLEDGEMENTS

This work is supported in part by the National Natural Science Foundation of China (NNSFC) with the Grants Nos. 11847216, 11675143, 11675145, and 11375153.

-
- [1] P. Dona, S. Speziale, arXiv:1007.0402.
 - [2] C. Rovelli and F. Vidotto, *Covariant Loop Quantum Gravity* (Cambridge University Press, Cambridge, 2014).
 - [3] C. Rovelli, L. Smolin, Nucl. Phys. B**442**, 593 (1995) .
 - [4] A. Ashtekar, M. Bojowald, J. Lewandowski, Adv. Theor. Math. Phys. **7**, 233 (2003).
 - [5] A. Ashtekar, P. Singh, Class. Quant. Grav. **28**, 213001 (2011).
 - [6] J. Yang, Y. Ding and Y. Ma, Phys. Lett. B**682** (2009) 1.
 - [7] A. Dapor, K. Liegener, Phys. Lett. B**785** (2018) 506.
 - [8] B.F. Li, P. Singh, A. Wang, Phys. Rev. D**97**, 084029 (2018).
 - [9] A. Ashtekar, J. Phys. Conf. Ser. 189:012003 (2009).
 - [10] A. Ashtekar, A. Corichi and P. Singh, Phys. Rev. D**77**, 024046 (2008).
 - [11] P. Singh, Class. Quant. Grav. **26**, 125005 (2009).
 - [12] A. Ashtekar and D. Sloan, Gen. Relativ. Gravit. **43**, 3619 (2011).
 - [13] L. Linsefors and A. Barrau, Phys. Rev. D**87**, 123509 (2013).
 - [14] M. Shahalam, M. Sharma, Q. Wu, and A. Wang, Phys. Rev. D**96**, 123533 (2017).
 - [15] M. Shahalam, M. Sami, and A. Wang, Phys. Rev. D**98**, 043524 (2018).
 - [16] M. Sharma, M. Shahalam, W. Qiang, A. Wang, JACP **11** (2018) 003.
 - [17] T. Zhu, A. Wang, K. Kirsten, G. Cleaver, and Q. Sheng, Phys. Lett. B**773**, 196 (2017).
 - [18] T. Zhu, A. Wang, G. Cleaver, K. Kirsten and Q. Sheng, Phys. Rev. D**96**, 083520 (2017).
 - [19] W.-J. Jin, T. Zhu, and Y. Ma, arXiv:1808.09643.
 - [20] B. F. Li, P. Singh, A. Wang, Phys. Rev. D**98**, 066016 (2018).
 - [21] B. Bolliet, A. Barrau, K. Martineau, F. Moulin, arXiv: 1701.02282 (2017).
 - [22] A. Bhardwaj, E. J. Copeland, J. Louko, arXiv:1812.06841.
 - [23] T. Zhu, A. Wang, K. Kirsten, G. Cleaver, and Q. Sheng, Phys. Rev. D**97**, 043501 (2018).
 - [24] Q. Wu, T. Zhu, and A. Wang, Phys. Rev. D**98**, 103528 (2018).
 - [25] K. Martineau, A. Barrau, and S. Schander, Phys. Rev. D**95**, 0835017 (2017).
 - [26] I. Agullo, A. Ashtekar, and W. Nelson, Class. Quant. Grav. **30**, 085014 (2013).
 - [27] I. Agullo, A. Ashtekar, and W. Nelson, Phys. Rev. Lett. **109**, 251301 (2012).
 - [28] I. Agullo, A. Ashtekar, and W. Nelson, Phys. Rev. D**87**, 043507 (2012).
 - [29] M. Fernández-Méndez, G. A. Mena Marugán, and J. Olmedo, Phys. Rev. D**86**, 024003 (2012).
 - [30] M. Fernández-Méndez, G. A. Mena Marugán, and J. Olmedo, Phys. Rev. D**88**, 044013 (2013).
 - [31] L. C. Gomar, M. Fernández-Méndez, G. A. Mena Marugán, and J. Olmedo, Phys. Rev. D**90**, 064015 (2014).
 - [32] L. C. Gomar, M. Martín-Benito, and G. A. Mena Marugán, Phys. Rev. D**93**, 104025 (2016).
 - [33] D. Martín-de Blas and J. Olmedo, JACP **1606** (2016) 029.
 - [34] M. Bojowald, G. M. Hossian, M. Kagan, and S. Shankaranarayanan, Phys. Rev. D**78**, 063547 (2008).
 - [35] T. Cailleteau, J. Mielczarek, A. Barrau, and J. Grain, Class. Quant. Grav. **29**, 095010 (2012).
 - [36] T. Cailleteau, A. Barrau, J. Grain, and F. Vidotto, Phys. Rev. D**86**, 087301 (2012).
 - [37] E. Wilson-Ewing, Int. J. Mod. Phys. D**25**, 1642002 (2016).
 - [38] E. Wilson-Ewing, Comptes Rendus Physique **18** (2017) 207.
 - [39] J. Mielczarek, Springer Proc. Phys. **157** (2014) 555.
 - [40] M. Bojowald and J. Mielczarek, JCAP **1508** (2015) 052.
 - [41] L. Linsefors, T. Cailleteau, A. Barrau and J. Grain, Phys. Rev. D**87**, 107503 (2013).
 - [42] B. Bolliet, A. Barrau, J. Grain and S. Schander, Phys. Rev. D**93**, 124011 (2016).
 - [43] B. Bolliet, J. Grain, C. Stahl, L. Linsefors and A. Barrau, Phys. Rev. D**91**, 084035 (2015).
 - [44] J. Grain, Int. J. Mod. Phys. D**25**, 1642003 (2016).
 - [45] I. Agullo, and N. A. Morris, Phys. Rev. D**92**, 124040 (2015).
 - [46] J. Mielczarek, L. Linsefors and A. Barrau, Int. J. Mod. Phys. D**27** (2018) 1850050.
 - [47] K. Martineau, A. Barrau, and J. Grain, Int. J. Mod. Phys. D**27**, 1850067 (2018).

- [48] T. Zhu, A. Wang, G. Cleaver, K. Kirsten, and Q. Sheng, *Int. J. Mod. Phys. A* **29**, 1450142 (2014).
- [49] T. Zhu, A. Wang, G. Cleaver, K. Kirsten and Q. Sheng, *Phys. Rev. D* **90**, 063503 (2014).
- [50] T. Zhu, A. Wang, G. Cleaver, K. Kirsten and Q. Sheng, *Phys. Rev. D* **89**, 043507 (2014).
- [51] T. Zhu, A. Wang, G. Cleaver, K. Kirsten, and Q. Sheng, *Phys. Rev. D* **90**, 103517 (2014).
- [52] T. Zhu, A. Wang, G. Cleaver, K. Kirsten, Q. Sheng, and Q. Wu, *JCAP* **10**, 052 (2015); T. Zhu, A. Wang, K. Kirsten, G. Cleaver, Q. Sheng, and Q. Wu, *JCAP* **03**, 046 (2016); T. Zhu, A. Wang, G. Cleaver, K. Kirsten, Q. Sheng, and Q. Wu, *ApJL* **807**, L17 (2015).
- [53] T. Zhu, Q. Wu, and A. Wang, arXiv: 1811.12612; J. Qiao, G.-H. Ding, Q. Wu, T. Zhu, and A. Wang, arXiv: 1811.03216; Q. Wu, T. Zhu, and A. Wang, *Phys. Rev. D* **97**, 103502 (2018); T. Zhu and A. Wang, *Phys. Rev. D* **90**, 027304 (2014).
- [54] T. Zhu, A. Wang, G. Cleaver, K. Kirsten and Q. Sheng, *Phys. Rev. D* **93**, 123525 (2016).
- [55] P. Singh, *Phys. Rev. D* **73**, 063508 (2006).
- [56] A. Ashtekar, T. Pawłowski and P. Singh, *Phys. Rev. D* **74**, 084003 (2006).
- [57] K. A. Meissner, *Class. Quant. Grav.* **21** (2004) 5245.